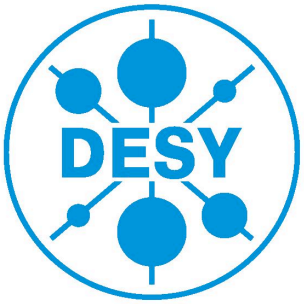

Study of vertex detector deformations using minivectors

Jasper Ryvers, University of Ghent, Belgium

Supervisor: Benjamin Boitrelle

September 8, 2015

Abstract

In this report, the effects that vertical deformations of MIMOMA26 sensors have on track reconstruction are studied. This happens for the double-sided setup of the PLUME collaboration using 2011 CERN π^- test beam data. Furthermore, a working model is discussed, whose goal is obtaining topological information of the sensor surfaces using minivectors only.

Contents

1 Introduction

At the end of this decade the International Linear Collider (ILC), a more than 30 km long e^-e^+-collider, will be built. The ILC will be a complementary collider to the LHC: the incoming particles will have well-defined quantum numbers and energy allowing for precision measurements, but the centre-of-mass energies that will be reached ($\sqrt{s} \approx$ 250-500 GeV) are a lot lower than those of the LHC. The projected luminosity will be in the range of $2 \cdot 10^{34}\ cm^{-2}\ s^{-1}$.
Although there will be only one interaction point, two different detectors will be used intermittently. The first is the SiD (Silicon Detector) and its name refers to a 1.2 m-tracker detector that consists solely of silicon. It is the most compact of the two and has a magnetic field of 5 T. The other one is the International Large Detector (ILD). Its 1.8 m-tracker integrates a TPC too. It will have a magnet that generates a 3.5 T-field. A design of the ILD is shown in Figure 1.

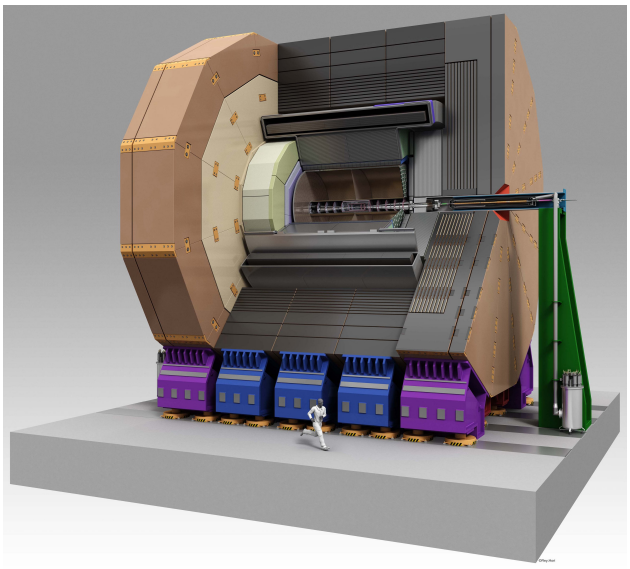

Figure 1: *The International Large Detector.*

In this report, the focus lies on the innermost part of the ILD, its *vertex detector*. Its projected hit resolution is 5 μm, corresponding to a standard deviation of $\sigma_{res} \approx 3\ \mu$m[1]. Furthermore, a proper design should reduce multiple scattering by reducing the material budget per layer to 0.1% of radiation length X_0. In Figure 2 one sees two possible designs for the vertex detector. The left proposal would consist of five single-sided layers, while the right one incorporates only 3 layers. These are however double-sided, so one has 6 sensor layers in total in this setup. It is this last design that plays a central role in research conducted by the PLUME collaboration, which this report is part of.

[1]The subscript 'res' stands for *residual*, a term that is explained in section 3.2.

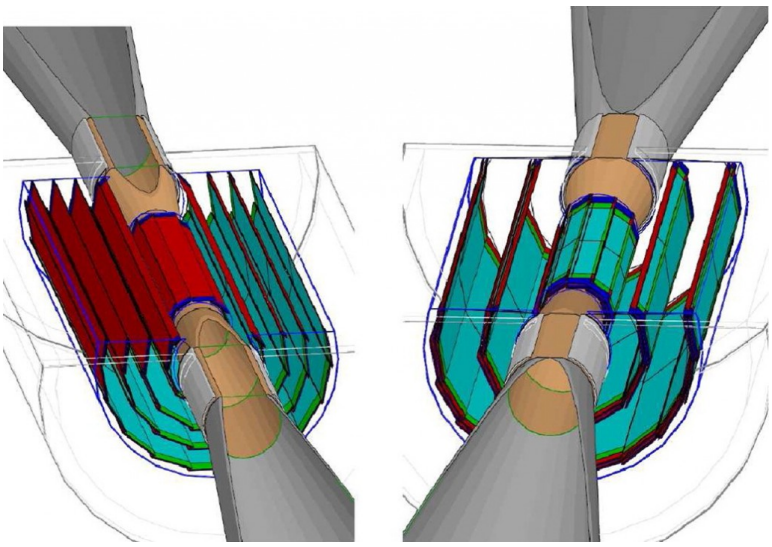

Figure 2: *Two ILD vertex detector designs. Left: 5 single-sided layers, right: 3 double-sided layers.*

2 PLUME

2.1 The collaboration

PLUME is an acronym for *Pixelated Ladder*[2] *With Ultra-low Material Embedding*[3], which summarizes the main research the collaboration is involved in: checking whether it is mechanically feasible to reach targets (close to those) that are outlined in [2]. The PLUME collaboration does this by designing, fabricating, and testing ladder prototypes that may be part of a vertex detector for a future linear collider.[4] The PLUME material budget goals are slightly more modest than outlined in [2]: 0.3% X_0 per double-sided layer, which makes for 0.15% per sensor layer. Partners that are involved in the collaboration include DESY Hamburg, IPHC[5], and the University of Bristol.

2.2 Design of a ladder prototype

In Figure 3 one can see how the final ladder will look like. Six sensors are mounted on a kapton flexible cable (constituting a *module*), and are separated by 2 mm of SiC foam from the other module. This foam was chosen because of its low fill factor, which unfortunately has the side effect of not making it very heat conducive. For prototypes of this ladder, MIMOSA26 sensors were chosen. These monolithic active pixel sensors are 50 μm thick. They were selected for their well-known behaviour, e.g. because they

[2]The term *ladder* refers to the evenly spaced MIMOSA sensors.
[3]*Plume* means 'feather' in French, referring to the light weight of the design.
[4]See also [1] for more information.
[5]Institut Pluridisciplinaire Hubert Curien, situated in Strasbourg.

were also used in the EUDET telescope. The MIMOSA26 sensors have an active area of 10.6 x 21.2 mm that is divided in 576 x 1152 square pixels. The pixel pitch is 18.4 μm. A top view of one module consisting of 6 sensors is shown in Figure 4.

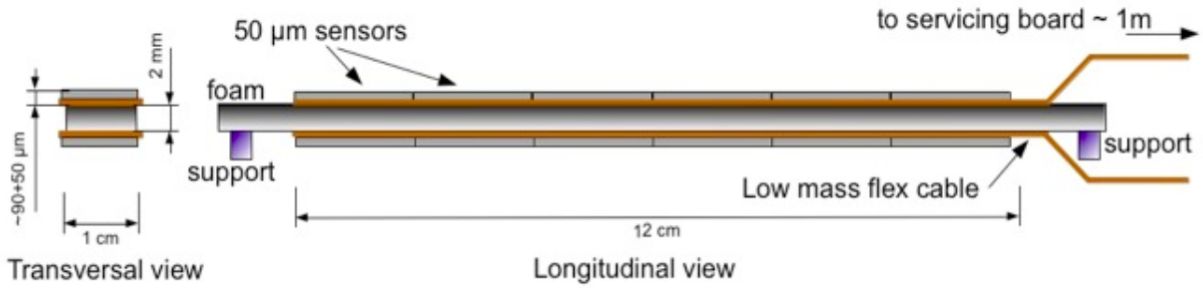

Figure 3: *General design of the ladder.*

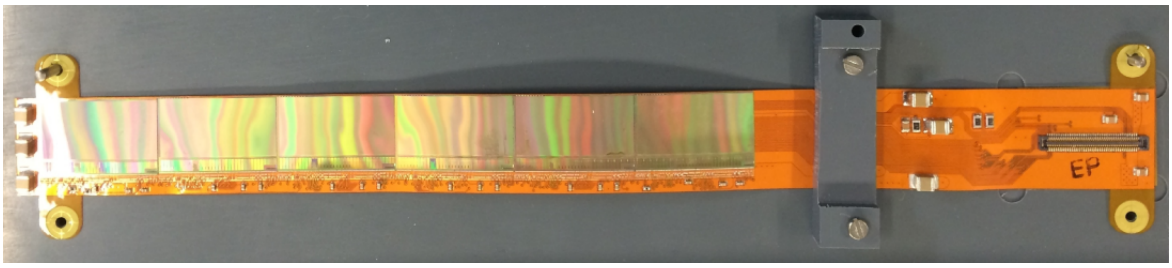

Figure 4: *A 2013 prototype of one module using copper tracings. [3]*

3 Test beam

3.1 Setup

In November 2011, the behaviour of the first prototype of the ladder (0.6% of X_0) was studied using a CERN SPS test beam consisting of 120 GeV π^-. For this report, a single run of two different configurations was studied. The configurations are shown in Figure 5. The prototype of the double-sided ladder can be found in the centre of each setup (green filling) and is in this context also referred to as the Device Under Test (DUT). Only two MIMOSA26 of each side were read out, because of a limitation of the data acquisition system. The red, horizontal bar is the incoming beam. It crosses two reference planes first, then passes through the DUT, and finally through two other reference planes. The left figure depicts the first configuration, in which the beam passes the DUT perpendicular to its surface. In the right setup, the DUT is tilted. The angle between the beam and the plane normal has a magnitude of 36°. Note that the only difference between both setups is this tilt: the threshold, airflow speed and other variables were kept constant.

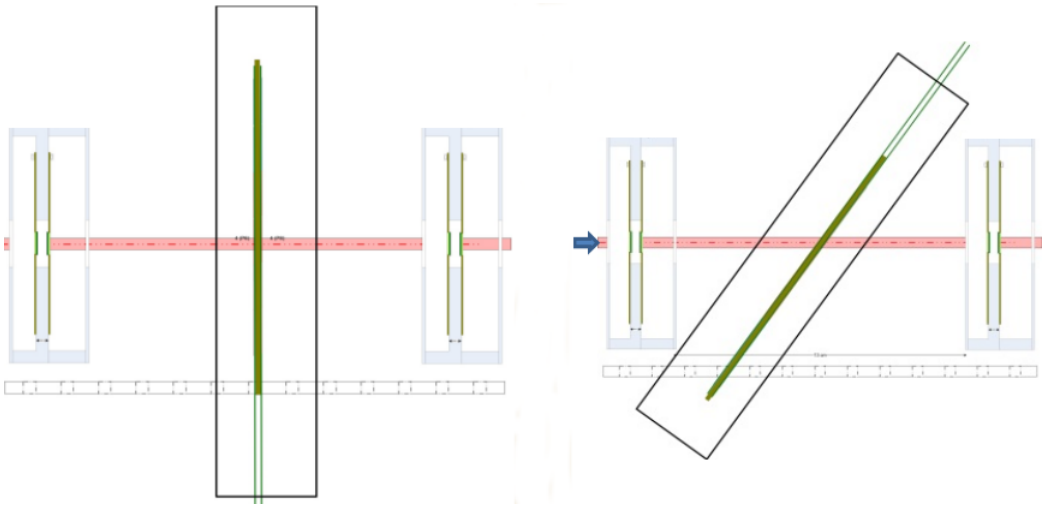

Figure 5: *Two test configurations. Left: DUT perpendicular to the beam, right: the DUT has a tilt of 36°.*

3.2 Track-hit residuals

The reference planes mentioned in the previous section play an important role. This is because a passing particle generates in each of these reference planes a hit. Based on these hits, a particle track prediction is made. If one now projects this track prediction onto the DUT, one arrives at an expected hit position (the red point in Figure 6). In reality however, one does not find a hit at exactly this spot. A registered hit that is nearest to it (the blue star in Figure 6) is then taken as the real DUT hit position. Summarizing: there is a difference between where one expects the particle track to cross the sensor and the measured DUT hit position. This difference is what is called a *track-hit residual*. The track-hit residual in the u-direction (also referred to as the *u-residual*) is noted as Δu.
One should take notice that we're working in the reference frame of a sensor mounted on the DUT, which is why the axes are named u, v, and w. The origin of this coordinate system is situated in the centre of the DUT plane and coincides in the ideal case with the origin of the (x, y, z)-lab system.[6]

[6]See also [4], section 4.1.6.

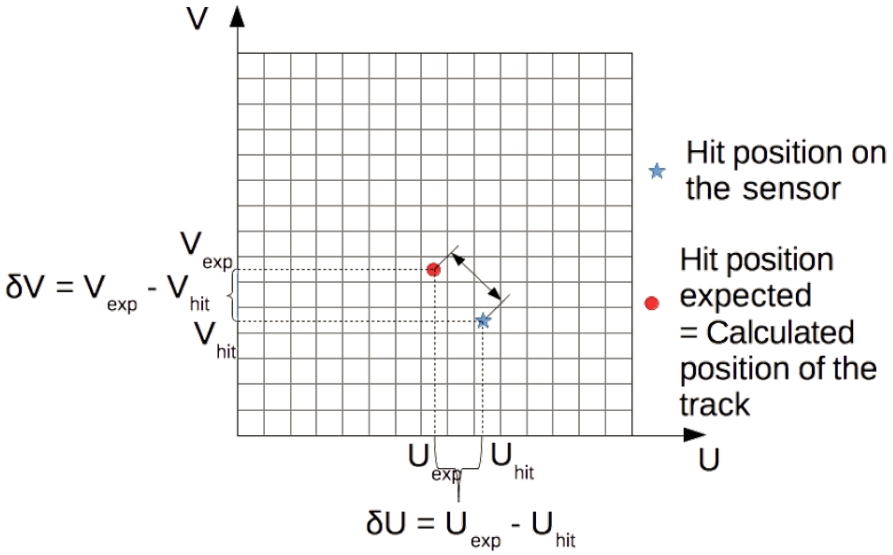

Figure 6: *Track-hit residuals in the uv-plane of a sensor.*

3.3 Test beam data

Introduction. The data of the beam was analyzed using TAF, a TAPI Analysis Framework which was developed by the IPHC.[5] The TAF software was for this report mainly used to correct for offsets or tilts relative to the primary reference plane. Plane offsets and tilts cause clear deviations in the data. This can be seen in Figures 7a and 7b for the perpendicular, first configuration.[7] A Gaussian fit to the u-residuals that is not centered at zero is a signature of an offset along the x-axis is, whereas a tilt about the z-axis is noticeable by the Δu-u correlation it causes. In the beginning the four reference planes were aligned and after that, alignment of the DUT planes followed.

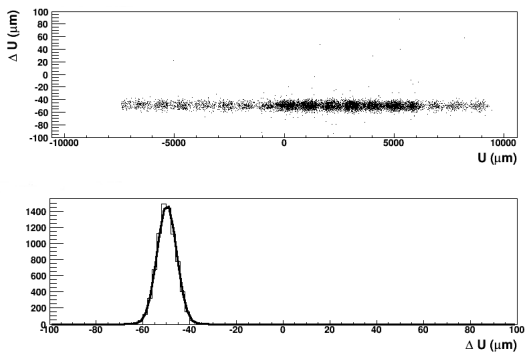

(a) *X-offset of 50 μm.*

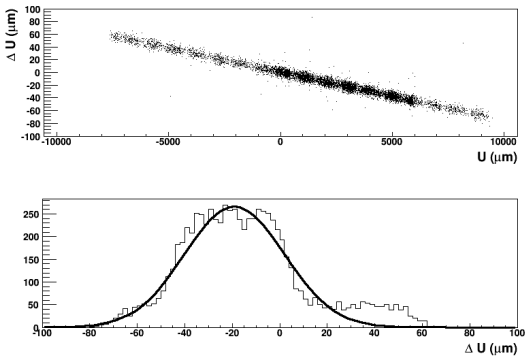

(b) *Tilt about Z-axis.*

Figure 7: *Effect of non-alignment on the data.*

[7] See also [4] for other examples of the effect of misalignment on residual data.

Configuration 1. If one corrects for all tilts and offsets in one run[8] of the perpendicular setup, one arrives at Figure 8.[9] The upper plot shows that there is almost no correlation between Δu and u, because if it were so, one would notice a tilt. The lower plot depicts the distribution of u-residuals. It is a Gaussian, centered at zero and having a standard deviation σ of 4.089 μm.
If one goes through the same correction procedure for a sensor on the other plane of the DUT, one arrive at a similar result. Because both planes are so close to each other, the data they produce is similar. Combining both data sets is advantageous as this reduces the standard deviation by a factor of $\frac{1}{\sqrt{2}}$.[10] The result is the distribution shown in Figure 9 and was generated by the MimosaMiniVectors-method, provided by the TAF software. Notice that σ is now only 3.266 μm, which approaches our desired 3 μm.[11]

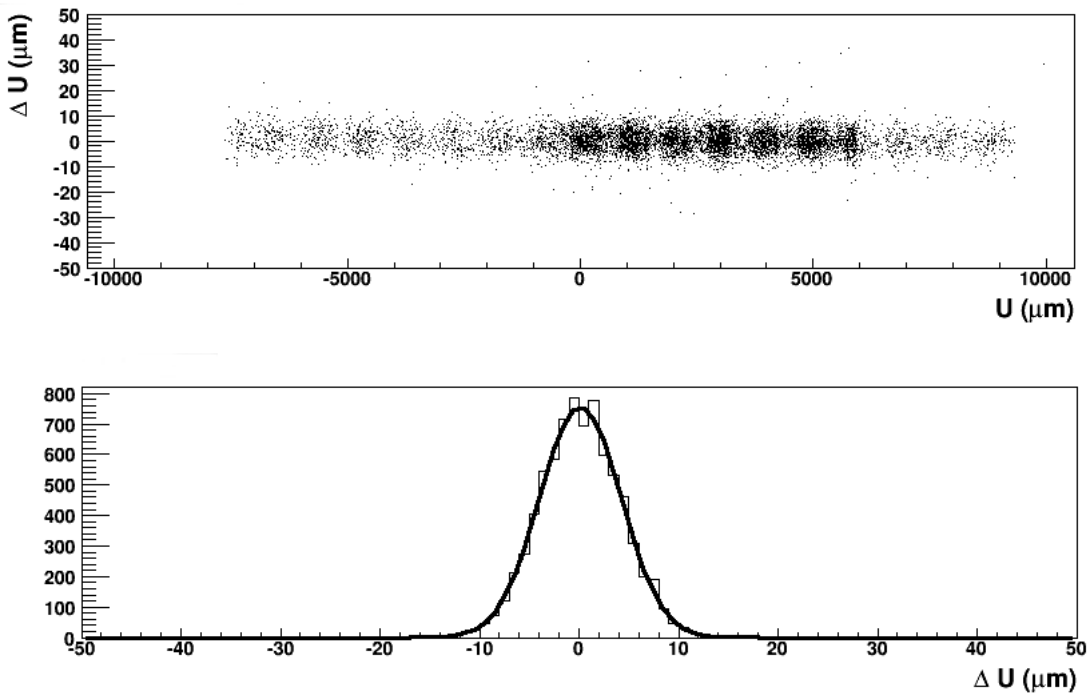

Figure 8: *Perpendicular setup, corrected u-residual data.*

[8] It was run 226056 that was studied.

[9] For comprehension, we restrict our attention to the residuals in the u-direction. In reality, the TAF software provides us with a lot more information that e.g. also show us the residuals in the v-direction and its correlation with sensor coordinates.

[10] A consequence of the Central Limit Theorem, which states that the standard deviation of the mean $\sigma(\bar{x})$ of N combined datasets that are independent but similar (i.e. having the same mean μ and variance σ) scales as $\frac{\sigma}{\sqrt{N}}$.

[11] Notice that $\sigma \equiv \sigma_{DUT} = \sqrt{\sigma_{res}^2 - \sigma_{ref}^2 - \sigma_{MS}^2} \neq \sigma_{res}$ (*ref* refers to the reference planes and the last negligible term to errors caused by multiple scattering), so one has to be careful when comparing σ_{DUT} and σ_{res}.

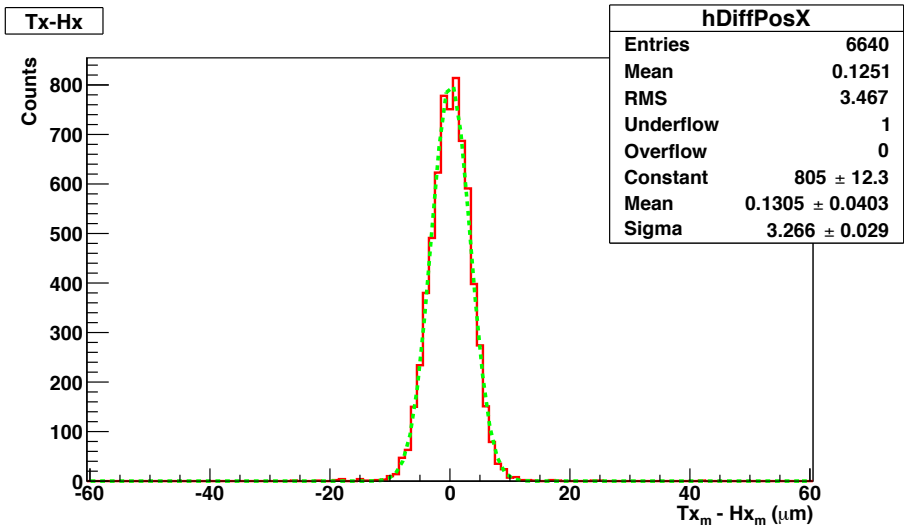

Figure 9: *The final curve after combining the two datasets.*

Configuration 2. If one goes through the exact same procedure as outlined above (correcting the residual data of the reference planes, next those of the DUT, and finally combining the DUT data to reduce σ) for run 226057 representing the 36°-tilted configuration about the v-axis, one gets slightly different results. Figure 10 shows the distribution of u-residuals for one of the MIMOSA26 sensors mounted on the DUT. The lower plot shows a Gaussian fit that has a relatively large σ of 6.065 μm. Furthermore, the optimization methods of TAF do not centre this fit at $\Delta u = 0$ μm. The upper plot however is more striking and reveals a banana-shaped curve instead of the expected horizontal line. Combining the data (Figure 11) in a like fashion reduces the standard deviation to 5.568 μm, which is a way too large number for PLUME's purposes.

Two questions should be posed here. First, why do we arrive at this strange correlational curve? Second, is it possible to find a way to reduce σ of the u-residual distribution for cases like these?

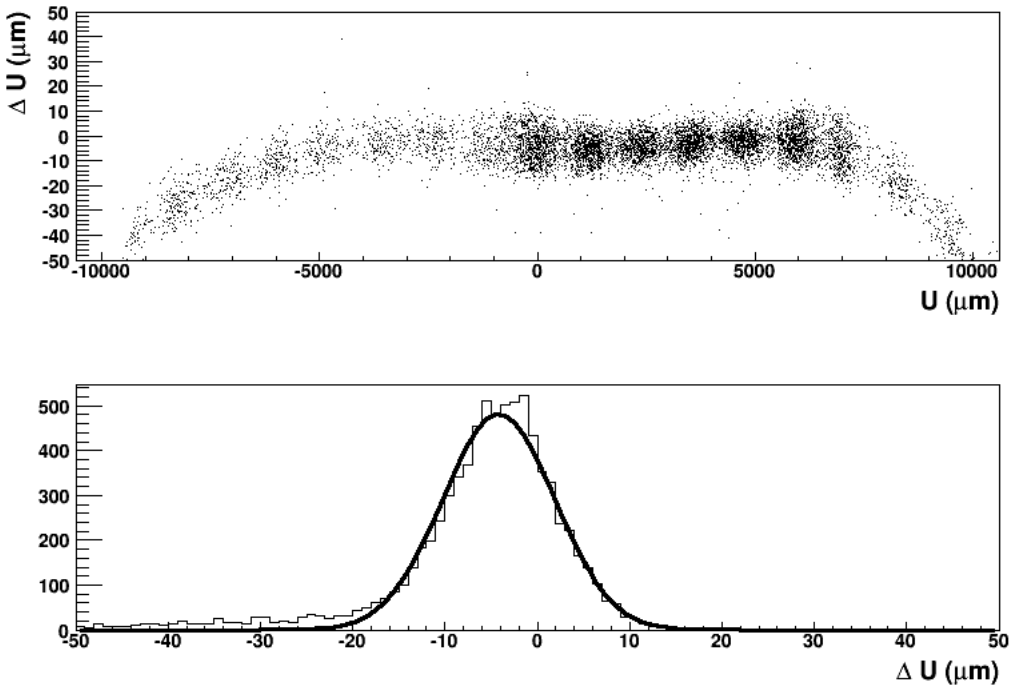

Figure 10: *Setup with a 36°-tilt about the v-axis, corrected u-residual data.*

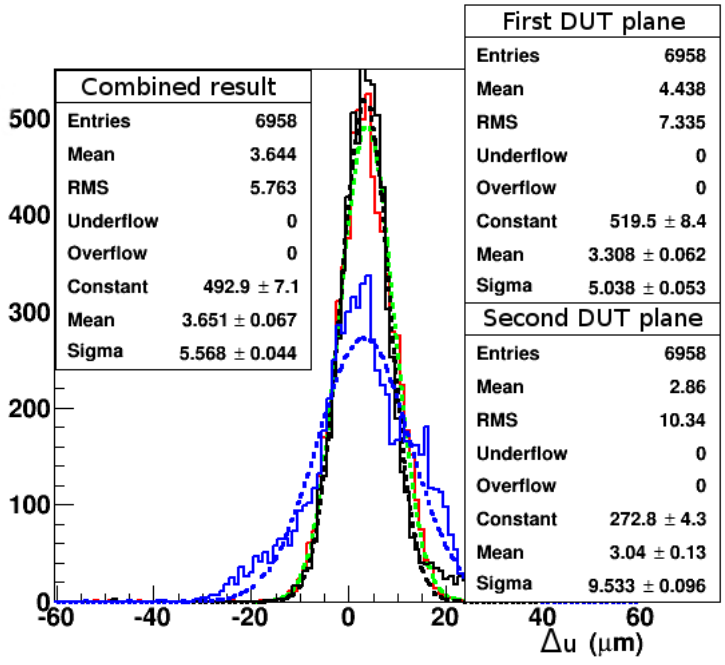

Figure 11: *Combining the data for the 36°-tilted setup.*

4 Vertical deformations

In the second configuration that was studied, we encountered a strange banana-shaped correlational curve, and this for a setup that is up to a tilted DUT essentially the same. In this section, the role vertical deformations have on the u-residuals is investigated. First, the geometry of vertical deformations is discussed and after that an outline is given sketching the connection with the minivector picture.

4.1 Geometry

Direct measurement performed by the University of Bristol have revealed that *the 50 μm-thick MIMOSA26 sensors deform vertically after they have been installed*. This happens because of mechanical constraints that can't be avoided, e.g. those caused by the glue points connecting the sensor to the module. In Figure 12 (see [5]) one can see that the surface of one ladder consisting of 6 MIMOSA sensors was completely mapped. The picture on the right gives us an estimate of the deformation magnitude, which is of the order of 10 μm.

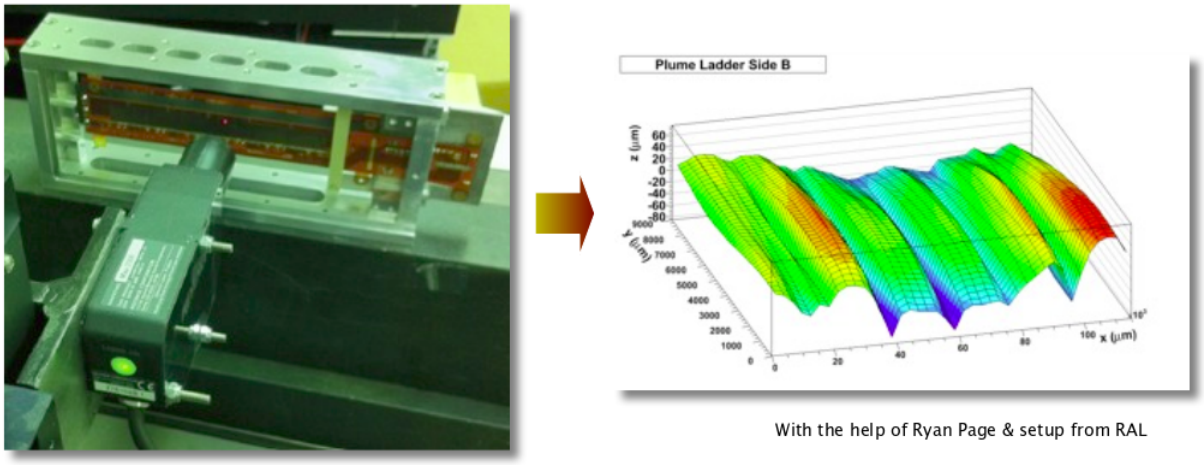

Figure 12: *Left: interferometry study of a ladder prototype, right: a map of the ladder surface.*

Figure 13 shows a sketch of a vertical deformation in the w-direction. The horizontal line represents the ideal flat plane, onto which one projects the predicted track position (u_h,w_{ideal}). The curved line represents a part of the deformed plane. Suppose an incoming particle crosses the deformed plane at (u'_h,w'_h). If one projects this real hit point on the ideal plane, one gets a reconstructed point (u'_h,w'_{ideal}). Repeating this procedure for each incoming particle, one clearly sees that one gets an non-zero Δu for each vertical deformation. Furthermore, one is able to deduce the following relation:

$\Delta u = tan\ \theta \cdot \Delta w$.[12]
And it is in this light that one can understand the strange correlational curve obtained previously in the second configuration (Figure 10, upper plot). In the correction procedure that was performed using TAF, it is implicitly assumed that the DUT planes are perfectly flat. But one can now see that every deviation of this planarity changes Δu and does that in such a way that a deformation upwards will make $\Delta u = u_{tr} - u_h$ more negative (u_h becomes larger), which is exactly the behaviour one notices on both sides of the banana-shaped curve in Figure 10.

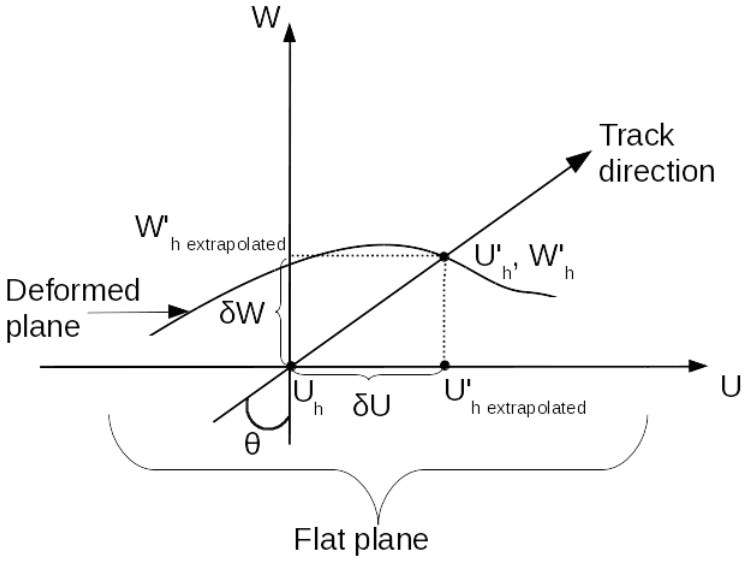

Figure 13: *A geometrical picture of deformations in the w-direction.*

4.2 Minivectors

If one extends the above geometrical picture to the double-sided ladder, one arrives at two reconstructed hit positions that are different from those based on the track prediction. If one now connects the two predicted hit positions and does so too with the reconstructed positions, one arrives at a *predicted* minivector $\vec{p}$ and a *reconstructed* minivector $\vec{r}$. Figure 14 illustrates these minivectors that are coloured green and red respectively. The horizontal curly brackets depict the u-residuals of both planes. Take note that the scale is completely wrong in Figure 14, because whilst both sides of the this setup are separated by as much as 2 mm, the vertical deformations of a sensor plane are only of the order of 10 μm.
Now for the remainder of this discourse, it is assumed that only the residuals in the u-direction Δu are relevant. This assumption is justified because whenever we mention

[12]This is a very useful equation (see also [6]), because based on the knowledge of θ and Δu, one can obtain the vertical deformation Δw starting from the u-residual data. Note also that if either Δw or θ are zero (incoming beam $\perp$ to the sensor), Δu should vanish.

tilting the detector plane, it is from now on done using the v-axis as rotation axis. One could also understand this as follows: if one would analyze a geometrical situation as in Figure 13 but now focus on the vw-plane, one would arrive at $\Delta v = tan\ \theta' \cdot \Delta w$. But θ' would be zero here, and so one arrives at $\Delta v = 0$ μm.

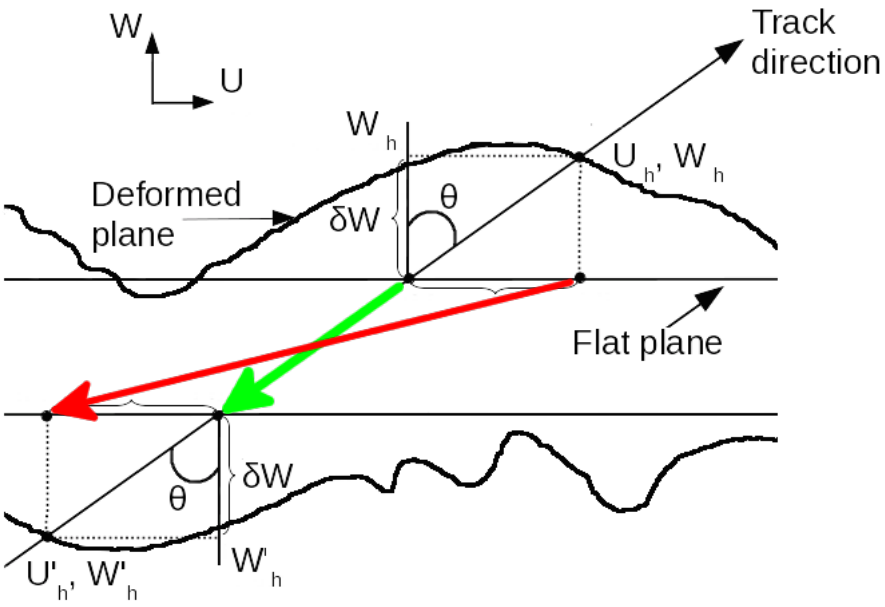

Figure 14: *An extended geometrical picture (not at the right scale). The green arrow represents the predicted minivector and the red one the reconstructed minivector.*

5 A simple model

In this final section, a simple model is discussed that tries to reproduce residual data and to obtain information of the deformed surfaces using minivectors only.
First, the workflow of the program is summarized. Next, some preliminary results are being discussed. Finally, an outlook is given that sketches possible extensions which might enable another approach to the problem at hand.

5.1 Procedure

The first step consisted of trying to copy the double-sided setup. Because we only wanted to study a part of the sensor, namely that one exposed most to the beam, we chose 3.3 mm as the magnitude of the u-interval. The separation of both planes is 2 mm. These two planes represent our *ideal* ones. We tried to limit the vertical deformations to 10 μm.

Planes were deformed randomly using ROOT's TRandom3 library[13] as to make different experimental setups. Each plane was 'deformed' by displacing it in the w-direction and by tilting it slightly. The rotation axis for the tilt was situated at the centre of each ideal plane. We refer to the deformed planes also as to the *real* planes.
Having thus generated a complete setup, the idea is to generate many particle tracks that have a set angle with the normal of the ideal planes, 36° in our case. Although the particle tracks cross the planes randomly, only those tracks that pass both real planes were selected.[14]
The final step consisted of determining the relevant minivector coordinates (or equivalently: Δu), based on where the track crosses both the ideal and the real planes. After that, all that remained was calculating a final quantity $\Delta Res_u := \Delta u_L - \Delta u_U$, the difference of the residuals of the lower plane Δu_L and of the upper one, Δu_U. This quantity was defined as to combine the residual data into one variable. In the minivector picture, it equals the first component of the difference of the predicted and the reconstructed minivector:

$$\begin{aligned}(\vec{p}-\vec{r})_u &= (u_{L,t}-u_{U,t})-(u_{L,h}-u_{U,h}) \\ &= (u_{L,t}-u_{L,h})-(u_{U,t}-u_{U,h}) \\ &= \Delta u_L - \Delta u_U.\end{aligned}$$

5.2 Preliminary results

Using this simple model, we give some preliminary results that arose from first tests of the program.
Figure 15 depicts a setup in which only the upper plane is 'deformed'. It has an downward offset in the w-direction of 1.81 μm and a clockwise tilt of about 15'. In this Figure, only the residuals of the upper plane are plotted. The distribution is difficult to interpret. We weren't able to compare this distribution directly to an experimental one, but the shape does not correspond to any residual data we encountered yet, which might indicate an error or an incomplete modelling of the physical situation.
The second plot depicted in Figure 16 does not show the number of u-residuals, but bins the quantity ΔRes_u instead. The generated configuration is random and one can see in the legend that both planes have an offset and are tilted.
In Figure 17, we approximate the deformed surface using a seventh order polynomial fit (see [3]) and use this fit as our deformed upper plane. The polynomials are slightly adapted Legendre polynomials[15]. The coefficients of the polynomials are listed in the

[13] This random number generator has period of about 2^{20000}.
[14] This restriction means that one is not able to draw tracks uniformly from the interval [0, 3300 μm]. Both a large beam angle and a large tilt may avoid a generated track from crossing both planes in the desired u-interval.
[15] The polynomials of order 2, 5, and 6 are respectively different from the Legendre ones because of a factor $\frac{1}{8}$ instead of one of $\frac{1}{2}$, $70x^4$ instead of $70x^3$, and $232x^6$ instead of $231x^6$. The other polynomials up to order 7 are Legendre ones.

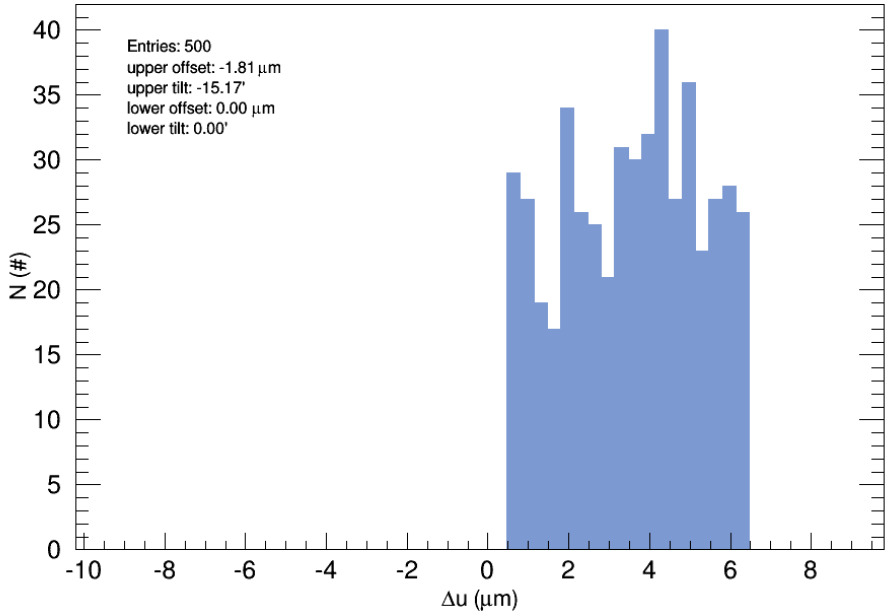

Figure 15: *Residuals of the upper plane in a simple setup.*

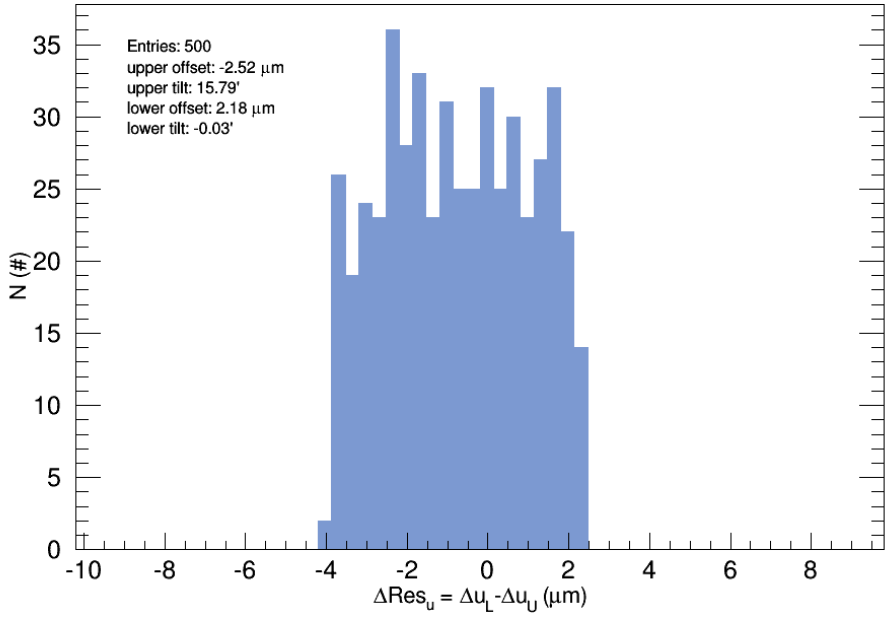

Figure 16: *The distribution of* ΔRes_u *for a random configuration.*

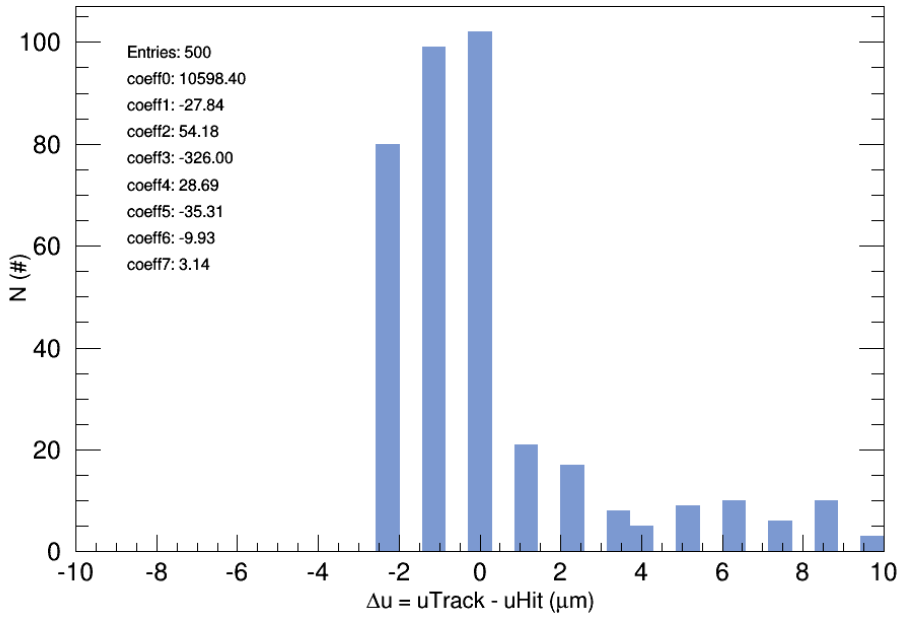

Figure 17: *Residuals of the upper plane for a polynomial fit to measured deformations.*

legend of Figure 17. The distribution has a distinct structure consisting of a central peak and a tail on the right side.

5.3 Outlook

The program that was written can be expanded in many ways.
A first step might be to 'explore' parameter space in a different way. Looking back, we think it might have been better to generate deformed planes in a stepwise fashion and not randomly. In this way, one would be able to scan configuration space more uniformously and thus to investigate more kinds of deformations.
Another step which should be taken is to make the model more realistic. The generated residual data would certainly be more valuable if one would make the deformed surfaces even more like those that were measured and mapped (see Figure 12) or if one would improve the beam model.
On a more practical note, saving the data should be made more efficient and convenient, and it would be a good thing too to save the generated data itself and not only bin it in a histogram format[16].
Comparing the generated data *to the experimental data* by quantitative means would be another achievement, and this especially for a histogram as in Figure 16. If one manages to get the beam data in such a histogram format, it would be possible to start an optimization procedure.

[16]Of which the appropriate bin width hasn't been found yet - another good reason to do so.

It would proceed as follows: define a cost function C [17] and try to approximate the experimental histogram as good as possible by an optimization procedure of choice. Once one finds an optimal generated histogram (i.e. that one which seems to minimize C), one is able to determine the optimal parameters that correspond to it. In the simple model outlined above, one would only be able to determine what offsets and tilts the experimental plane setup has. In a more extended version however, one might also obtain the coefficients of functional approximative terms (as in Figure 17).
The final goal could then be attained by using this topological information to map the real sensor surfaces and correct the residual data by 'shifting' the track prediction points in the w-direction appropriately. In the minivector picture, this comes down to letting the reconstructed minivector approach the predicted minivector. One is then at last able to reduce the residuals in the u-or v-direction.

6 Discussion

It was shown that vertical deformations of the order of only 10 μm have a considerable effect on residual data of 50 μm-thick MIMOSA26 sensors in a tilted configuration. These sensor deformations are inevitable and are caused by mechanical constraints. A working model was developed that could lead to an alternative way to map and correct for these surface deformations, a process which in the end could help improve the spatial resolution of the double-sided PLUME ladder.

[17] The obvious choice would be a cost function $C(G, D) = \Sigma_i (G_i - D_i)^2$, where G_i represents the i'th bin value of the generated histogram and D_i that of the histogram based on the data.

References

[1] PLUME Collaboration: Ultra-light ladders for linear collider vertex detector, Nuclear Instruments and Methods in Physics Research A 650, p. 208-212, Elsevier (2011). *A Nomerotski et al.*

[2] The International Linear Collider, Technical Design Report, Volume 4: Detectors (2013).

[3] Mid-term review of the second year (June 2015). *B. Boitrelle*

[4] CVD Diamond Sensors for Particle Detection and Tracking, dissertation, section 4.1.7 (January 1999). *D. Meyer*

[5] Ultra-light double-sided ladders for a LC vertex detector (October 2013). *I. Gregor*

[6] Alignment of the CMS tracker with LHC and cosmic ray data, section 8 (August 2014). *The CMS Collaboration*